Chapter 7

Porous Selective Laser Melted Ti and Ti6Al4V Materials for Medical Applications

Leszek A. Dobrzański,
Anna D. Dobrzańska-Danikiewicz,
Anna Achtelik-Franczak, Lech B. Dobrzański,
Marek Szindler and Tomasz G. Gaweł

Additional information is available at the end of the chapter

http://dx.doi.org/10.5772/65375

Abstract

This chapter characterises scaffolds manufactured in line with the make-to-order concept according to individual needs of each patient. The clinical data acquired from a patient during computer tomography, nuclear magnetic resonance or using traditional plaster casts is converted by a computer into a virtual solid model of a patient's loss. The model, through the multiplication of a unit cell, is converted into a porous model on the basis of which an actual object is manufactured with the method of selective laser melting (SLM) from Ti/Ti6Al4V powders. The created scaffold is characterised by good mechanical properties, which is confirmed by the results of the performed tensile and compressive strength tests. The material is additionally subjected to surface treatment consisting of the deposition of atomic layers of titanium dioxide with nanometric thickness.

Keywords: porous materials, scaffolds, CAMD, SLM, ALD, mechanical properties

1. Introduction

Additive manufacturing technologies are proliferating and becoming increasingly popular across various industries nowadays. Owing to their benefits, they support the development of multiple disciplines in the field of engineering wherever a clear need exists to fabricate elements with a complicated shape, geometry and a distinctive structure. Such elements include individualised implants, representing living tissues, closely accommodated to a given patient based on the results of computer tomography or nuclear magnetic resonance or traditional plaster casts.

Porous structures are much desired in medicine, especially where a porous element is to replace a missing bone. In such a situation, the task of the fabricated element is to stimulate a regeneration process of the adjacent bone tissue through an osteoconductive and osteoinductive activity. Osteoconduction is a process of bone loss regeneration consisting of the in-growth of osteoblasts—which are bone-forming cells originating from the adjoining bone stock—into the porous implant. In osteoinduction, though, the differentiation of mesenchymal cells is stimulated in the environment of osteoblasts. The cells represent a connective embryonic tissue occurring only in the embryonic period, from which all types of connective tissues, bone tissue, cartilage tissue and muscle tissue are created. In order for titanium scaffolds fabricated with SLS technologies to fulfil their role well in a patient's organism, they should be characterised by the appropriate size of pores, appropriate porosity, as well as strength permitting usage in bone implants functioning as scaffolds, which become a substructure and a support for the bone growing into them. Literature data shows [1–12] that the size of pores allowing the development of the bone growth process into the created scaffold, varies between the minimum of 50–200 μm and the maximum of 500 μm and the porosity of such a scaffold should not exceed 50%. A satisfactory result of a manufacturing process of porous titanium materials is seen when an element is achieved with open pores, characterised by an appropriate level of porosity and sufficiently good strength properties, which should be similar to the corresponding properties of a living bone tissue. Bone porosity is referred to as the volume fraction of the fluid phase filling the pore space of a bone in a given bone volume unit. The bone fluid phase consists of blood vessels together with blood, nerve fibres, bone cells and extracellular bone fluid. A cortical bone has the density of 1.99 g/cm^3. It has the longitudinal compressive strength of 131–224 MPa and the longitudinal bending strength of 79–151 MPa. The transverse compressive strength of a cortical bone is 106–133 MPa and bending strength is 51–56 MPa [13, 14].

Additive manufacturing enables to create objects with the final shape while allowing to control the manufactured element in each part of its volume. An advantage of AM technologies, as compared to competitive fabrication methods of porous materials with space fillers [10–12], is also an ability to fabricate without applying costly and time-intensive casting moulds, as a result of which the product achieved does not contain external admixtures which are often present in cast products. The maximum possible reduction of wastes generated in a manufacturing process as compared to waste-generating machining is ranking AM technologies higher than traditional manufacturing processes applied until now. The entire additive manufacturing process takes place in an atmosphere of inert gas, which prevents the creation of unwanted products of the reactions occurring between a material used for fabrication of elements and air components. Selective laser melting (SLM) technology, due to its advantages, is very well suitable for manufacturing in line with the make-to-order concept of individualised craniofacial implants, including palate implants.

2. Computer-aided materials design

An additive manufacturing process carried out with the SLM technique begins at the sage of computer design of 3D models of objects planned to be manufactured in reality. The key

http://dx.doi.org/10.5772/65375

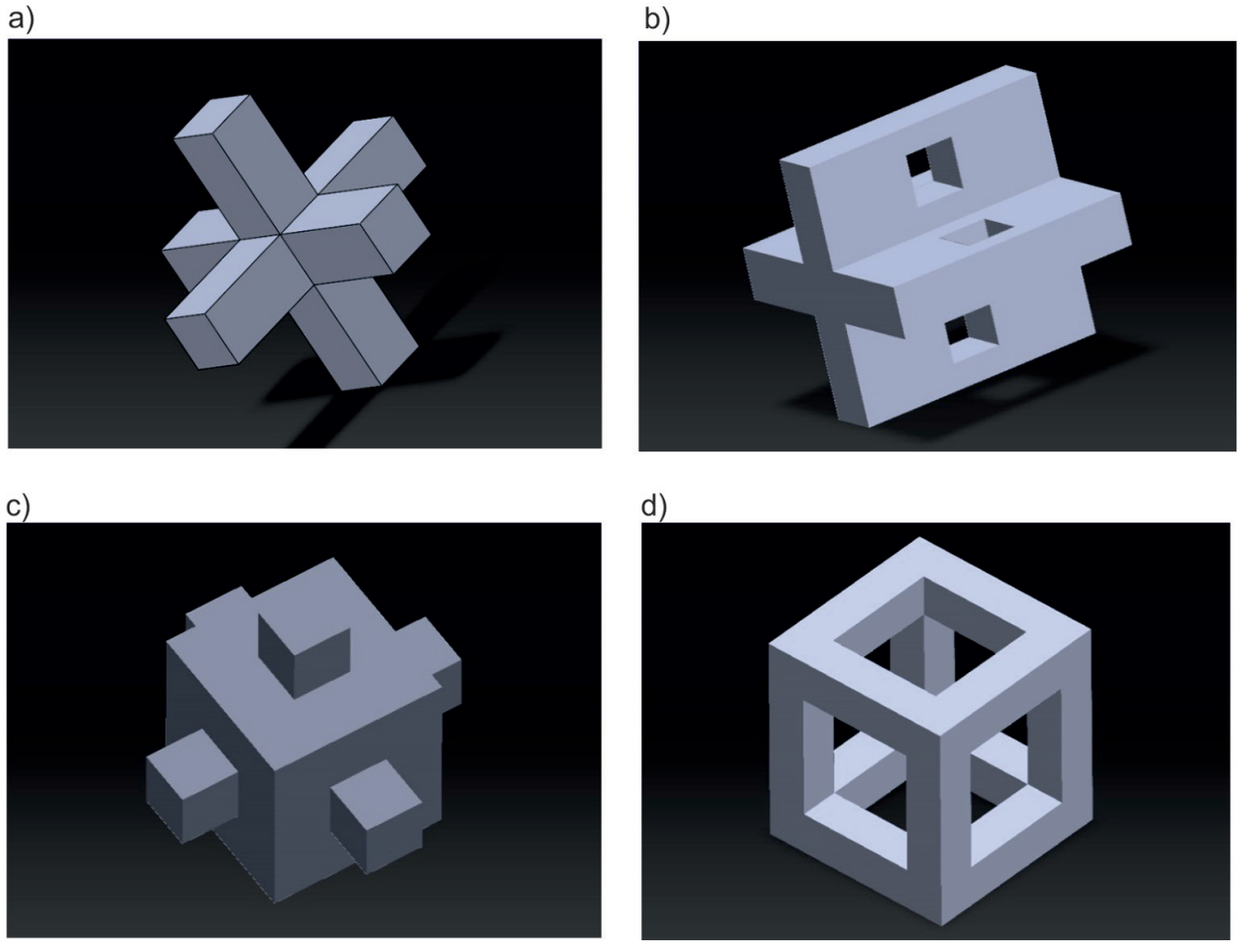

Figure 1. Unit cells according to a custom design: (a) type A: spatial cross; (b) type B: cross with openings; (c) type C: cube with tongues; (d) type D: cube skeleton.

benefit of the concept is that no constraints exist as to the shape and filling of a virtual model at the design stage; it allows representing an anatomical structure of organs, bones and human and animal tissues very accurately [15–20]. One of the specific aspects in this domain, being the subject of a series of experiments performed by the authors of this chapter, is the designing and manufacturing of porous biomimetic implants replacing a patient's palate loss. The loss may result from a genetic defect or a mechanical injury, or a neoplasm. A palate implant designed individually for each patient is a scaffold, the structure of which is made of open pores. A porous structure is to ensure appropriate growth conditions on the surface of pores for living cells by ensuring availability of nutrients. The computer-aided design of virtual models is preceded by a clinical stage at which accurate data is acquired from a patient regarding a 3D shape and dimensions of one's palate loss. The data can be acquired in the course of examinations conducted with computer tomography or nuclear magnetic resonance, or with traditional plaster casts, the shape of which is then transferred to a computer with a 3D scanner. Regardless the option chosen, the outcome of such activities is a virtual solid implant model of a palate which is further processed into a porous model.

A unit cell which, when multiplied many times, will create a porous scaffold structure, is required to create a virtual porous palate implant. A unit cell can be chosen from the avail-

able database being part of commercial software or it can be individually designed according to individual preferences. When designing a unit cell, it is significant to model it in such a way that it is symmetrical relative to all the axes of symmetry, which guarantees the correct transformation of a virtual solid model into a porous model, without errors on the created lattice. Unit cells according to a custom design are shown in **Figure 1**. All the designed unit cells inscribe themselves into a cube with the side of 500 μm. A type A cell (**Figure 1a**) has the shape of a spatial cross with arms with the dimensions of 100 × 100 μm. A type B cell (**Figure 1b**) is a cross with its arms 100 μm thick and has small quadrangle openings in such arms with the side of 100 μm. A type C cell (**Figure 1c**) is a cube with the side of 300 μm, on each wall of which tongues are arranged symmetrically in the form of smaller cubes with the side of 100 μm. A type D cell (**Figure 1d**) is a skeleton of a cube with the sides equal to 100 μm.

A solid implant model and the applied unit cell are saved in *stl* files before a virtual solid model of a piece of a palate loss is transformed into a virtual porous model. The extension is needed so that the model is transferred to a device carrying out a selective laser sintering

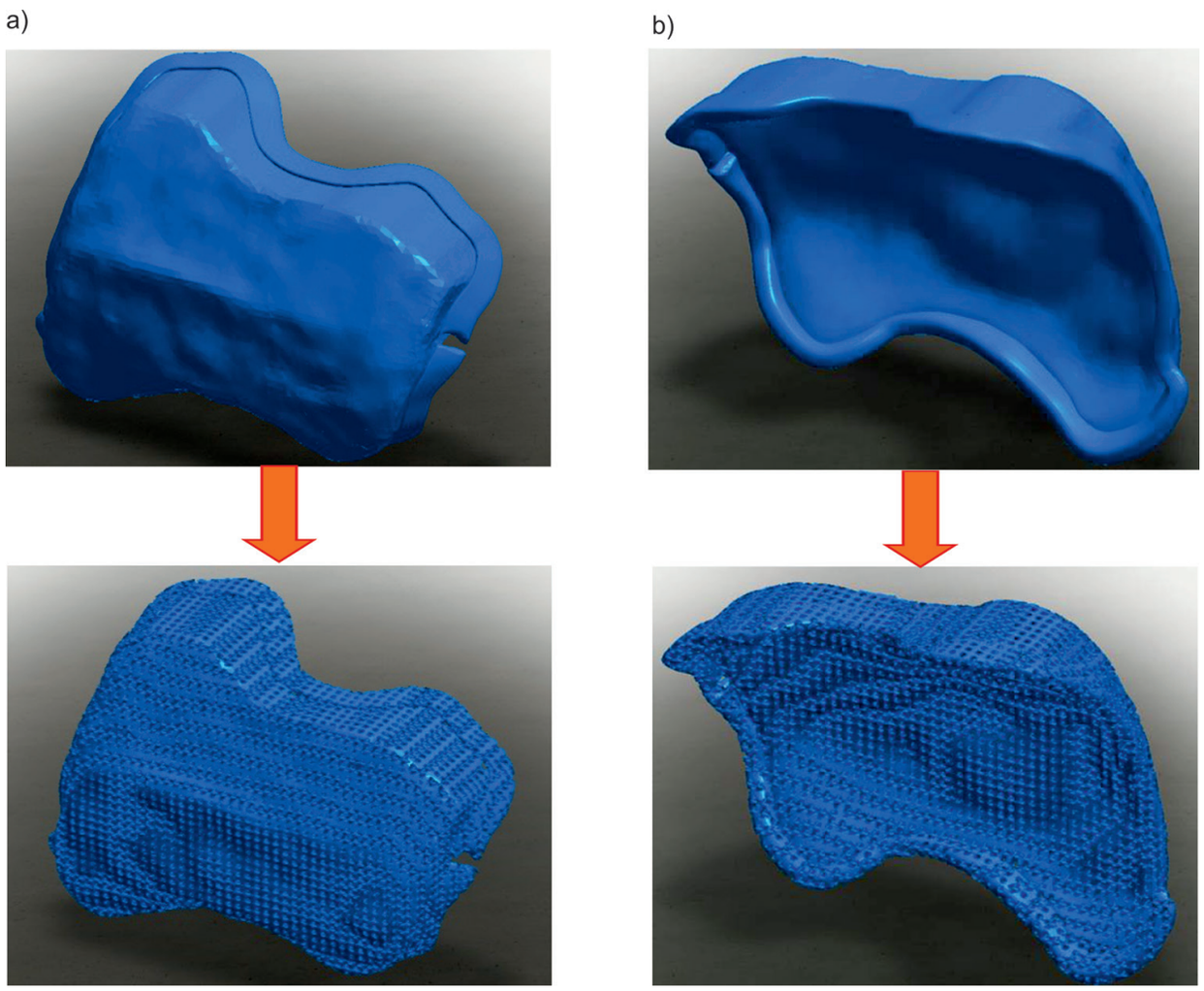

Figure 2. Virtual solid implant model and a corresponding porous model created after transformation: (a) top view; (b) bottom view.

http://dx.doi.org/10.5772/65375

(SLM) process. This ensures the automatic conversion of a virtual scaffold model into a model made of the net of triangles with the standard size of the area of a single triangle creating a net which is predefined directly by CAD software. It is possible to control the size of the area of a single triangle to densify the net, thus to control the accuracy of surface representation of an element produced having a complicated shape. If the field of a single triangle is decreased when converting the model into a net of triangles, accuracy is increased, but also the process is extended, both, at the stage of multiplication as well as at the stage of object fabrication. Highly efficient, latest generation software must therefore be used for very high accuracies. A virtual porous model created after transformation with a specifically designed structure composed of multiplied unit cells, has geometrical dimensions perfectly corresponding to the model from before the transformation (**Figure 2**).

3. Selective laser melting of scaffolds

Pristine titanium and Ti6Al4V titanium alloy, which, as per the international standard [21], is dedicated to biomedical applications, is a material used for the fabrication of actual objects which are to act as individualised palate implants. Titanium is classified as a light metal with a density of ρ = 4507 g/cm^3, a melting point of 1668°C and boiling point of 3260°C. It occurs in two allotropic variants, i.e. α and β. The α titanium variant has a hexagonal lattice (A3), which, at the temperature of 882.5°C, is converted into a high-temperature variant β crystallising in the regular system (A2). Pristine titanium occurs in the single-phase variant α and the titanium alloy Ti6Al4V in the double-phase variant α and β [22–24]. Titanium possesses high mechanical strength relative to the mass; however, its essential properties, allowing to employ it in medicine, include high biocompatibility with living tissues and pitting corrosion resistance, intercrystalline corrosion resistance and stress corrosion resistance. An input material in the form of powder must be used for the selective laser melting technology. Pristine titanium powder with the grain size of 0–45 μm and titanium Ti6Al4V alloy powder with the grain size of 15–45 μm, with the chemical composition consistent with the manufacturer's specification shown in **Table 1**, were used in the course of the experiments carried out to fabricate actual objects. The results of the qualitative chemical composition analysis performed with the EDS method (**Figure 3**) confirm the presence of the elements stated by a manufacturer in technical and commercial specifications. Powder grains in the both cases are spherically shaped, which is observable in microscopic photos (**Figure 4**).

Pristine titanium and titanium Ti6Al4V alloy powders are an input material from which porous implants for medical uses are manufactured in a selective laser sintering process. Preparatory measures are taken before the actual manufacturing process, during which, after

Powder	Al	V	C	Fe	O	N	H	Others total	Others each	Ti
Ti	–	–	0.01	0.03	0.14	0.01	. 0.004	. <0.4	. <0.01	Remainder
Ti6Al4V	6.35	4.0	0.01	0.2	0.15	0.02	0.003	≤0.4	≤0.1	

Table 1. Fraction of particular chemical elements in composition of powders subject to experiments in per cents.

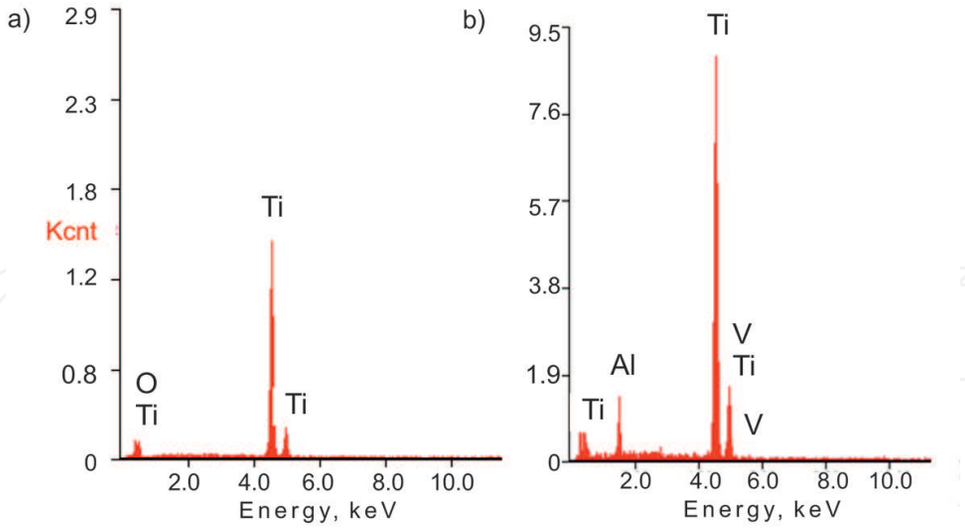

Figure 3. Results of qualitative chemical composition analysis: (a) pristine titanium; (b) TiAl6V4.

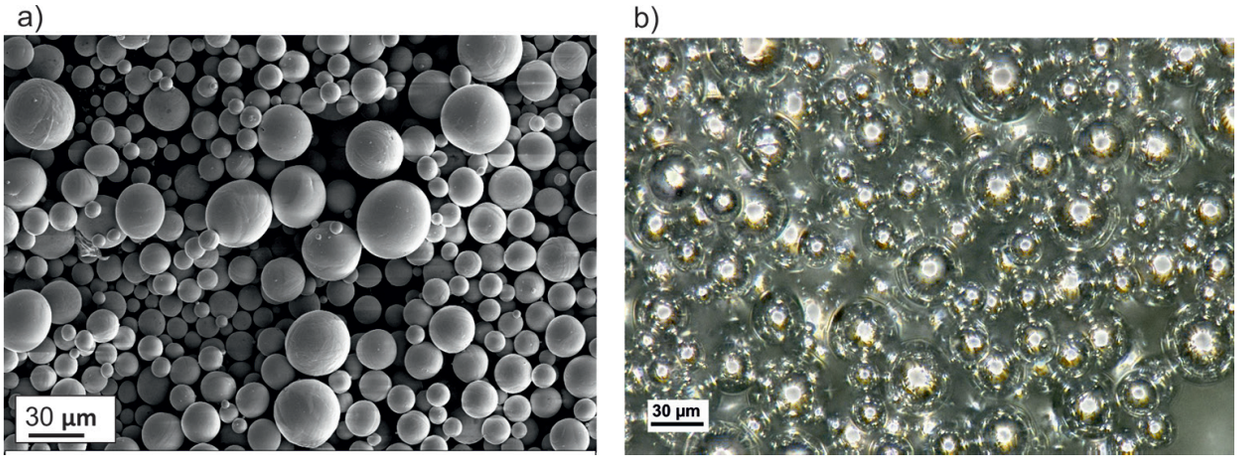

Figure 4. Powders used in laser sintering process: (a) pristine titanium; SEM image; (b) Ti6Al4V titanium alloy; image from stereoscopic microscope.

transferring a 3D virtual scaffold model to an SLM device, the virtual object is placed in a working chamber in the adequate position, i.e. on the relevant edge and under the right angle. The selection of the adequate virtual model position in a working chamber is an important aspect due to the following factors: the amount of powder needed to carry out a manufacturing process once, the mechanical properties of the scaffolds produced [25] and the number of supports needed to generate scaffolds. The purpose of the supports is to support the produced actual object and to secure it against collapse under its own weight. In the next stage, the virtual model is divided into layers parallel to the working platform surface of the device on which it is to be manufactured. The number of layers depends on the parameter set by the operator, i.e. powder layer thickness to be given before each melting. The following manufacturing conditions are also selected prior to commencing a fabrication process of an actual object: laser power, scanning rate, distance between consecutive remelting paths and the laser

http://dx.doi.org/10.5772/65375

beam diameter. Before starting the selective laser melting process, titanium powder is heated in a vacuum in the surrounding of shielding gas at an elevated temperature (160–200°C) to remove any moisture from the powder, as necessary.

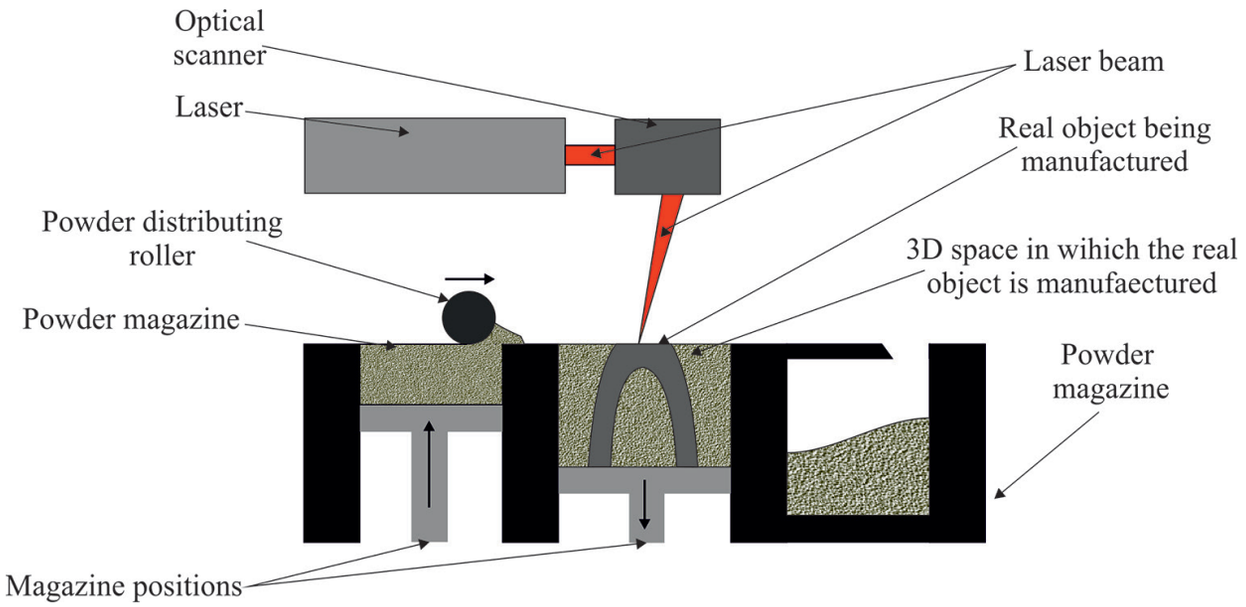

Figure 5. Schematic of the Selective Laser Melting (SLM) device; an own picture prepared on the basis of Refs. [26–28].

The actual selective laser melting process serves to produce metallic scaffolds encompasses the selective melting of powders point after point and layer after layer using a high-power laser [30–34] with a device the diagram of which is shown in **Figure 5**. A process of object manufacturing by SLM was carried out from the bottom, i.e. from the working platform side. Each layer produced is adhering to the preceding one until the process is completed [35, 36]. Powder is fed from a magazine holding loose material and is then distributed with a specific quantity with a shaft travelling across a working platform, which is descending by the exact height of the layer being sintered, whose thickness corresponds to one layer of virtual 3D model section. The excess powder is collected with a roll to a second empty magazine. A computer-controlled laser beam is melting the powder (**Figure 6**) in a specifically predefined manner and in selectively picked points. A powder layer is deposited and melted selectively in an alternate fashion, until the entire, permanently integrated real object is created. The excess powder, removed from a working platform, can be re-used, by collecting it into a separate special magazine, after being finely sifted in subsequent fabrication processes [37, 38]. An example of a scaffold observed with a bare eye, whose size matches the palate loss of one of the patients participating in clinical trials, is shown in **Figure 7**, showing, respectively, view from the top (**Figure 7a**) and from the bottom (**Figure 7b**). This scaffold, manufactured using Ti6Al4V titanium alloy powder, was removed mechanically from the working platform and supports were removed.

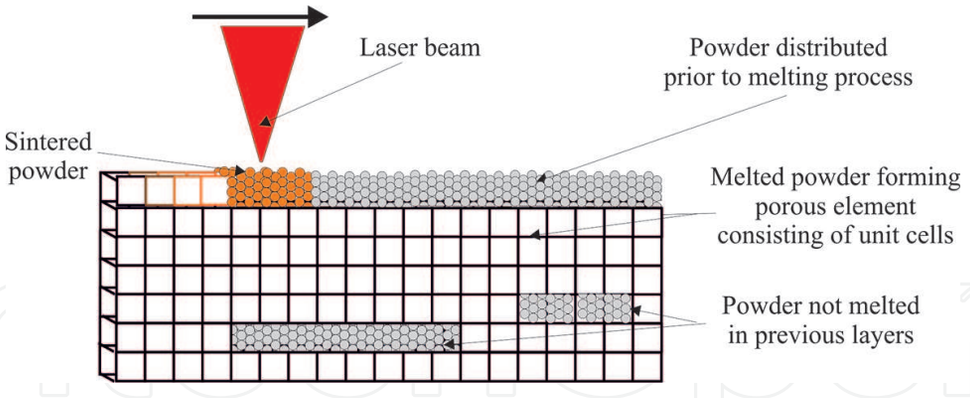

Figure 6. Sintering of individual powder layers in SLM process [29].

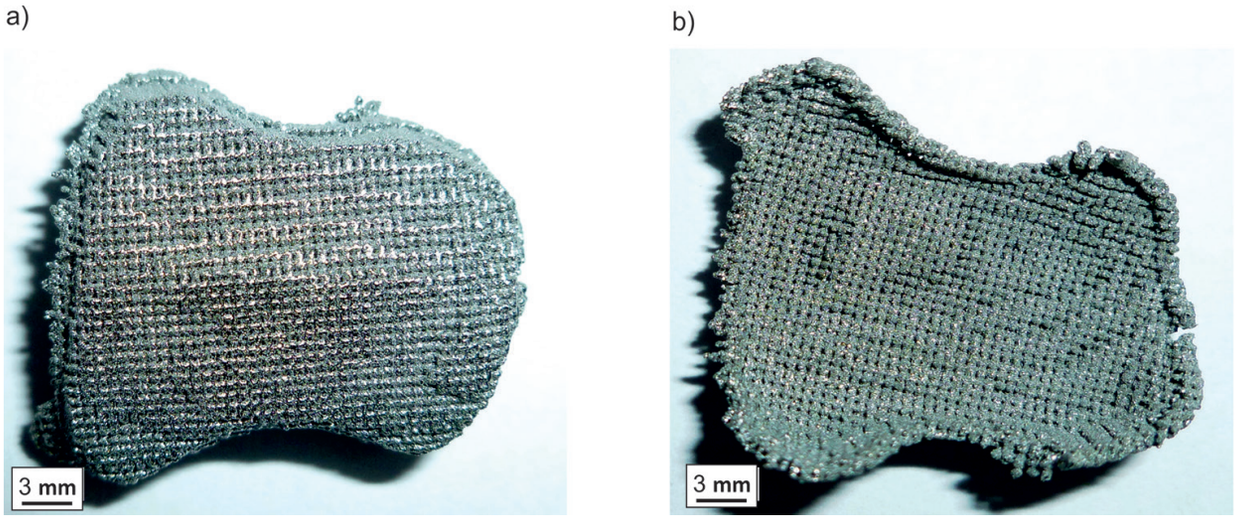

Figure 7. Example of scaffold manufactured with SLM method from Ti6Al4V powder, whose shape matches the palate loss of a patient: (a) top view; (b) bottom view.

The scaffolds created were subjected to microscopic observations using a scanning electron microscope. It was observed that the surface topography of the created scaffolds shows a porous, regular latticework-shaped structure. It was also found that the pores of the scaffolds produced are open, which was one of the designers' key assumptions due to the fact that this material, acting as an implant, is to grow through a patient's living tissue. Microscope observations of the studied material's surface topography indicate also the presence of singular, spherically shaped powder grains on its surface, which were deposited there due to adhering to the scaffold surface remelted in an SLM process. **Figure 8** shows a surface topography of the scaffolds manufactured with Ti6Al4V powder with the SLM method using the pre-produced virtual models comprised of multiplied unit cells created by the author, of, respectively, type A (**Figure 8a**), type B (**Figure 8b**), type C (**Figure 8c**) and type D (**Figure 8d**).

http://dx.doi.org/10.5772/65375

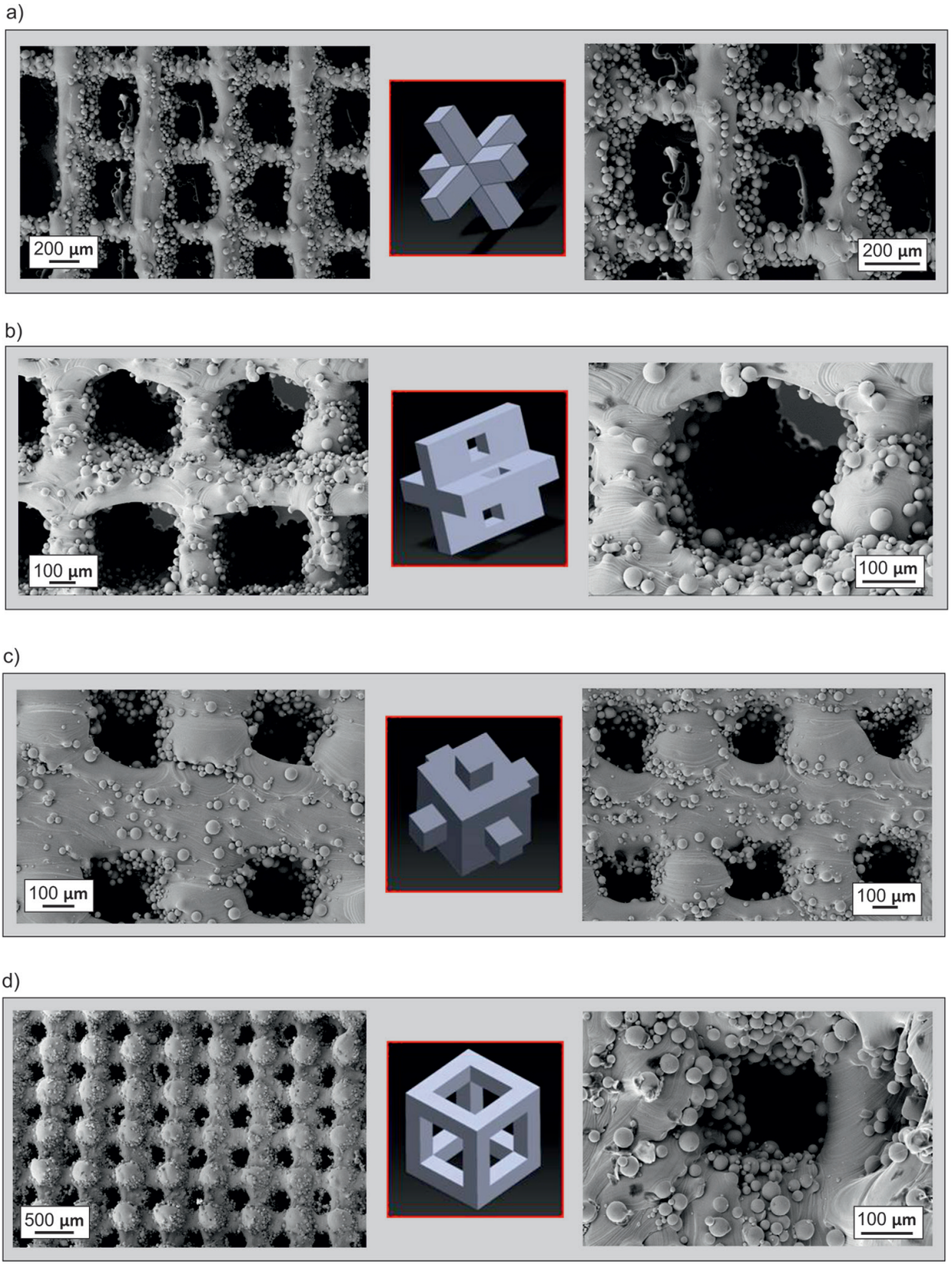

Figure 8. Surface topography of scaffolds manufactured as multiplication of units cells of type A (a), type B (b), type C (c) and type D (d).

4. Mechanical properties of scaffolds

On the one hand, scaffolds are made of robust materials such as pristine titanium and Ti6Al4V titanium alloy and on the other hand, they have a distinct structure consisting of open pores and possess interesting mechanical properties such as tensile and compressive strength. The tensile strength of material is determined according to the dependency (Eq. (1)) [39], using for calculations the results of strength tests determining the maximum tensile strength and a known field area of the sample cross section. The dependency (Eq. (2)) [39] allows to calculate the compressive strength of material using data such as the maximum compressive strength values obtained during strength tests and the sample cross section. The shape and dimensions of the samples designed to perform tensile and compressive strength tests are shown in **Figure 9**.

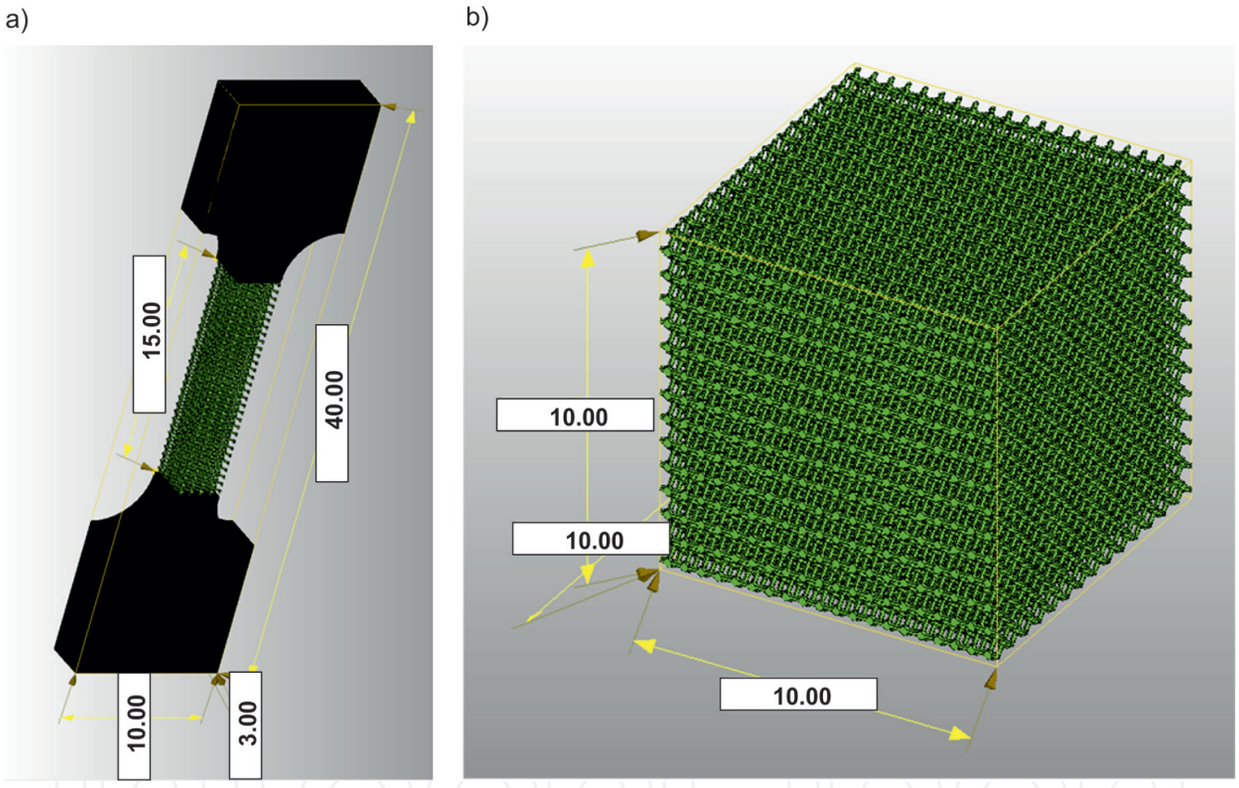

Figure 9. Samples for strength tests designed by computer: (a) for tensile strength; (b) for compressive strength.

Strength test type	Field area of sample cross section (mm²)	Material	Maximum force acting on sample (N)	Strength (MPa)	
				R_m	R_c
Tensile strength test	9	Ti	324	36	
		Ti6Al4V	423	47	
Compressive strength test	121	Ti	15 125		125
		Ti6Al4V	27 346		226

Table 2. Results of tensile and compressive strength tests made for scaffolds produced with Ti and Ti6Al4V powders (values in the table rounded to integers).

http://dx.doi.org/10.5772/65375

$$R_m = \frac{F_m}{S_0}\left[\frac{N}{m\,m^2} = MPa\right] \quad (1)$$

$$R_c = \frac{F_m}{S_0}\left[\frac{N}{m\,m^2} = MPa\right] \quad (2)$$

where:

R_m — tensile strength;

R_c — compressive strength;

F_m — maximum force acting on the sample and

S_0 — field area of cross section of sample.

The strength properties of scaffolds depend on the size of their pores, laser path curve and unit cell arrangement in the space of a system of coordinates [25]. **Table 2** shows the results of experiments made after selecting the optimum conditions of executing a manufacturing process, such as the size of scaffold pores of 250 μm, a laser path with an improved curve and unit cell arrangement at the angle of 45° relative to the axis of abscissa of the system of coordinates.

The average tensile strength value of laser-sintered scaffolds of Ti6Al4V powder is 47 MPa and is over 30% higher than the strength of scaffolds produced in the same conditions using pristine titanium powder, as presented in **Figure 10**. The characteristic of progression of tensile curves proves that both the porous titanium and porous Ti6Al4V titanium alloy are elastic-plastic materials with a clearly marked elastic strength and yield strength. Similar as in the case of tensile strength, a scaffold made of titanium alloy possesses much higher compressive strength than a titanium scaffold. The difference is much higher, though, because the compressive strength of the material made of Ti6Al4V is 225 MPa and is 80% higher than the compressive strength of a titanium sample (120 MPa). **Figure 11** shows charts presenting a dependency between compressive stress and deformation for the porous materials sintered with a laser using, respectively, Ti and Ti6Al4V powders.

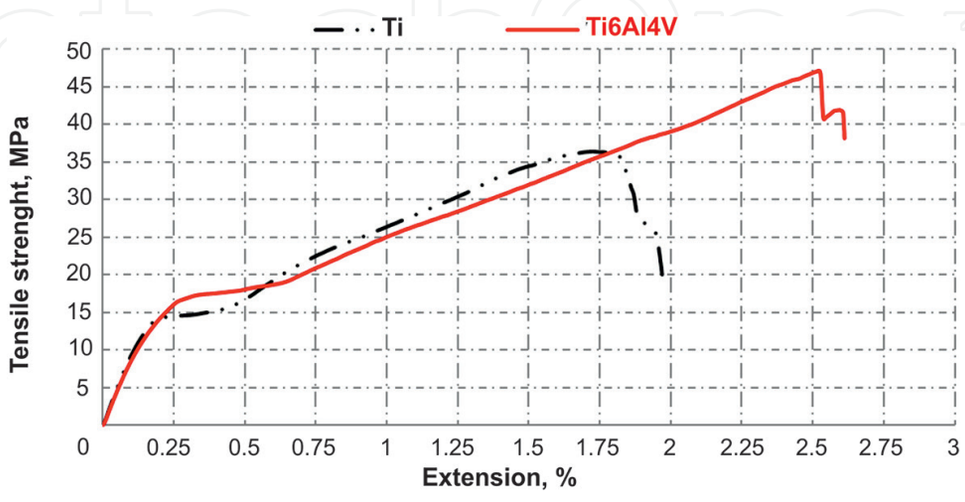

Figure 10. Dependency between tensile stress and extension recorded for porous materials sintered with laser from Ti and Ti6Al4V powders.

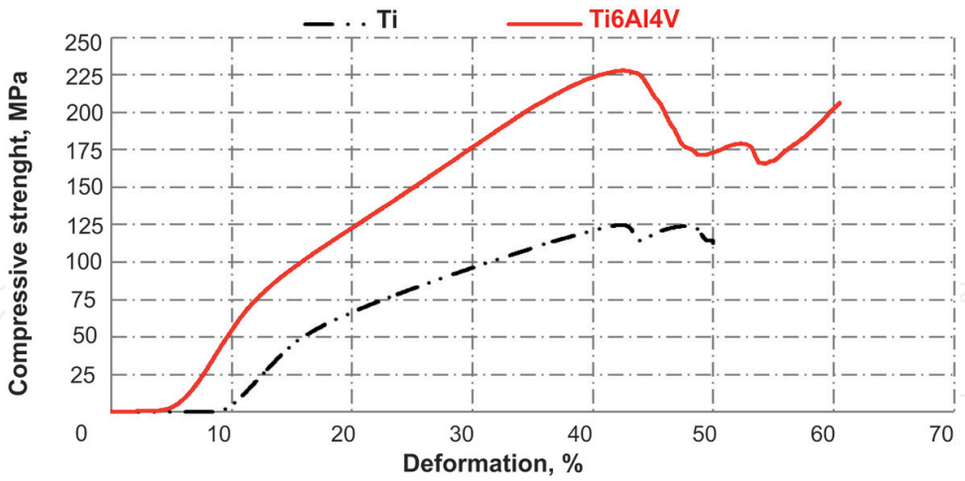

Figure 11. Dependency between compressive stress and deformation recorded for porous materials sintered with laser from Ti and Ti6Al4V powders.

5. Atomic layers of dioxide titanium deposited onto scaffolds' surface

Pristine titanium and its Ti6Al4V alloy, of which scaffolds are made which are to act as implants of palate fragments, are the materials broadly used in medicine as implants due to their low density, a beneficial strength-to-yield stress limit ratio, good corrosive resistance and biocompatibility. A further improvement in those materials' properties such as biotolerance and osteoconduction is possible by employing surface treatment. Thin layers are depos-

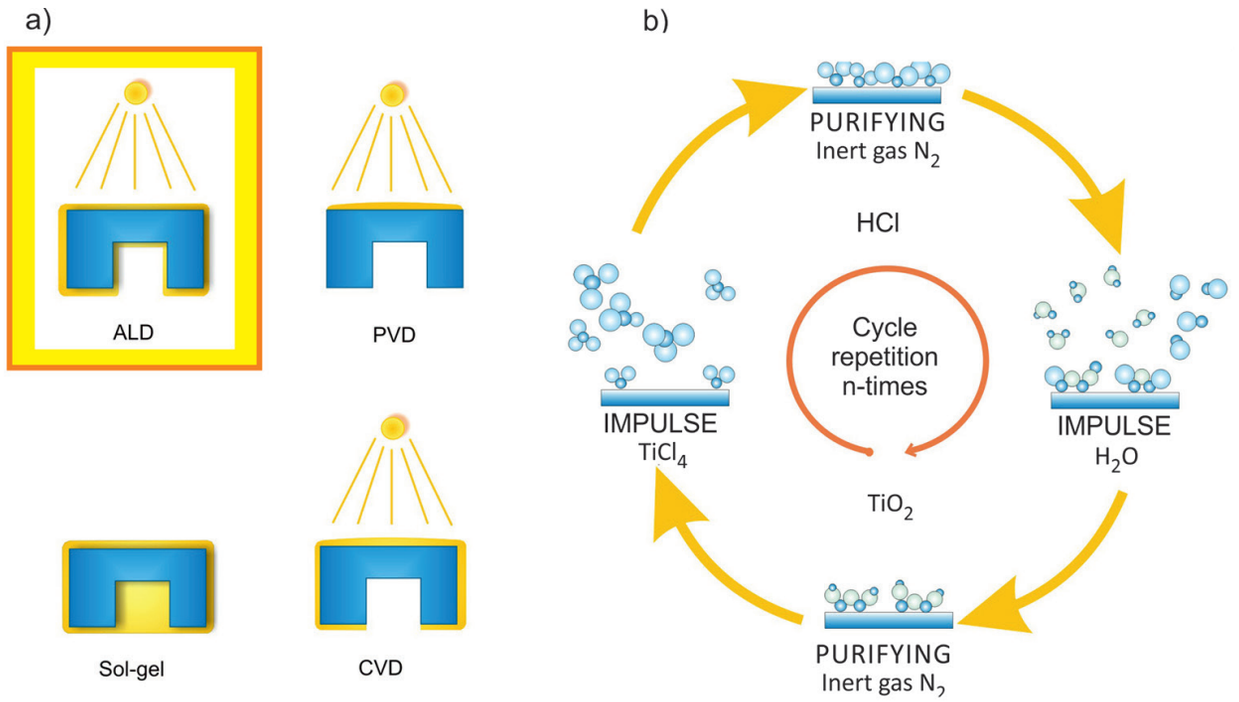

Figure 12. Atomic layer deposition: (a) ALD method versus other methods; (b) process cyclicity.

http://dx.doi.org/10.5772/65375

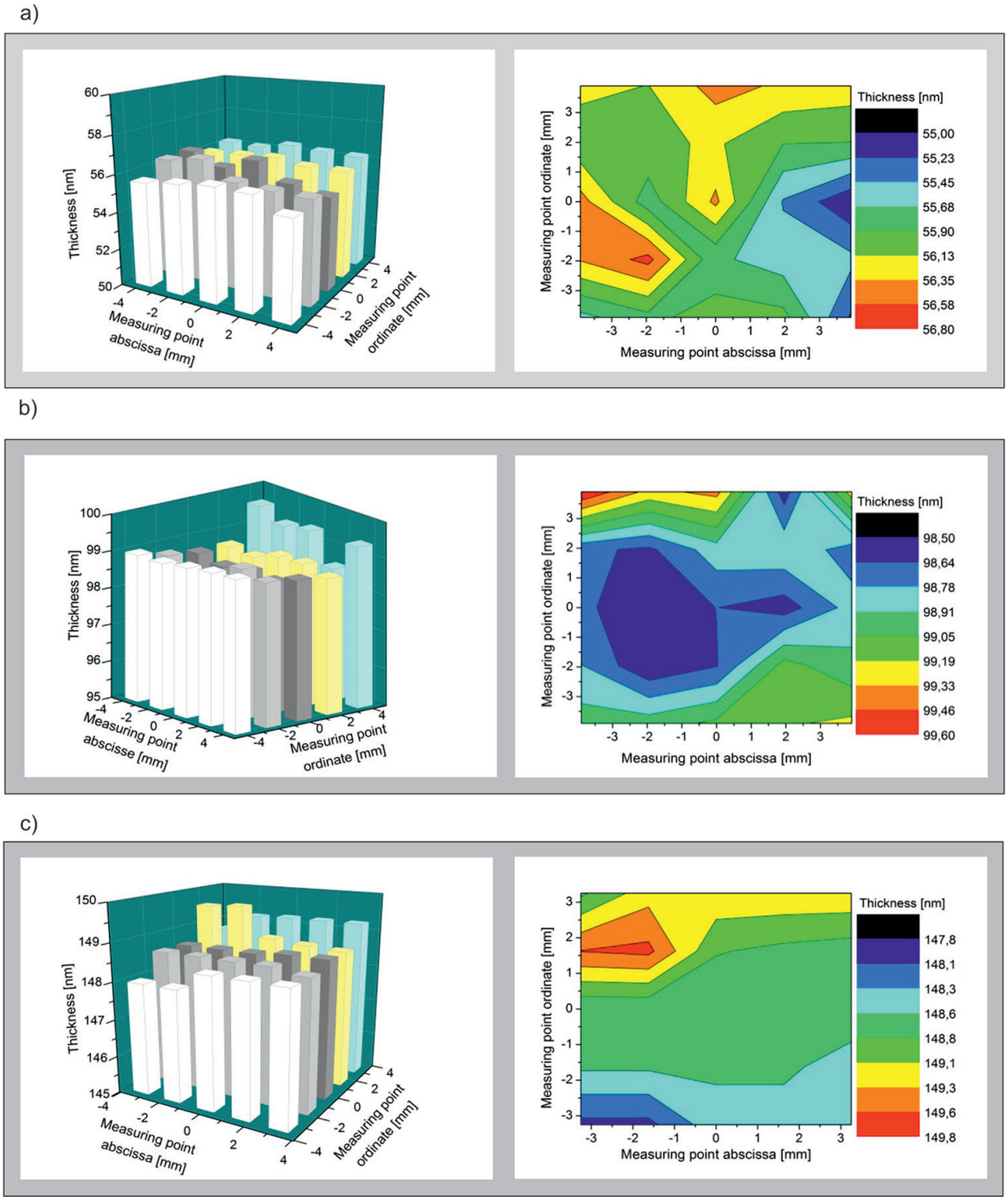

Figure 13. Layer thickness and thickness distribution map of TiO_2 layered deposited by ALD for: (a) 550 cycles; (b) 1050 cycles; (c) 1550 cycles [44].

ited permanently onto the surface of implants made of metallic biomaterials intended for long use in a human organism, most often with the following methods [40–43]: plasma sputtering, electrophoresis, physical vapour deposition (PVD) and chemical vapour deposition (CVD),

sputter coating and electrochemical deposition. Where layers are deposited onto the surface of porous biomaterials with complicated shapes, it is very important to be able to accurately control the growth mechanisms enabling to constitute a very thin layer with its thickness measured at a nanoscale, but most of all, it is essential to be able to deposit geometrically complex areas uniformly. One method, i.e. atomic layer deposition (ALD), gives such an opportunity now, as shown in **Figure 12a**, against optional methods. The ALD method is a variant of the CVD method characterised by the cyclic use of alternate precursor pulses with strong reactivity with a chamber purged with inert gas between such pulses (**Figure 12b**). By applying strongly reactive precursors, which—after supplying them into a chamber—are reacting immediately with a substrate by forming a monolayer and preventing a further reaction, each cycle increases the layer thickness by a strictly specified value within the range of 0.01–0.3 nm. The number of cycles performed preconditions the final thickness of the deposited layer. The authors of this chapter, in the course of their own works, have performed a series of experiments consisting of the deposition of atomic TiO_2 layers onto scaffolds sintered from Ti/Ti6Al4V and have carried out for this purpose, respectively, 550, 1050 and 1550 cycles.

The ALD technique enables to deposit a chosen chemical compound more uniformly across the entire surface of the part being treated, also if this part has a porous structure, as is the case with scaffolds. The thickness of the layers deposited by ALD is determined with a spectroscope ellipsometer equipped with special software. The average thickness of layers deposited by ALD technique for the said cases of 550, 1050 and 1550 cycles is 55.95, 98.90 and 148.73 nm, respectively. The difference in the thickness of the deposited TiO_2 layers on the studied area does not exceed 2 nm, which can be analysed in detail by studying layer thickness distribution maps. The best results were obtained for a layer deposited in 1050 cycles. A difference in the thickness of the deposited layer in this case does not exceed 1.1 nm across the entire area of the surface-treated item. Bar charts for each number of cycles, presenting the thickness of the deposited TiO_2 layer in the particular measuring points and the corresponding layer thickness distribution maps, are shown in **Figure 13**.

Changes in sample colour depending on the number of the executed ALD cycles, hence depending on the thickness of the deposited TiO_2 layer, is an interesting phenomenon

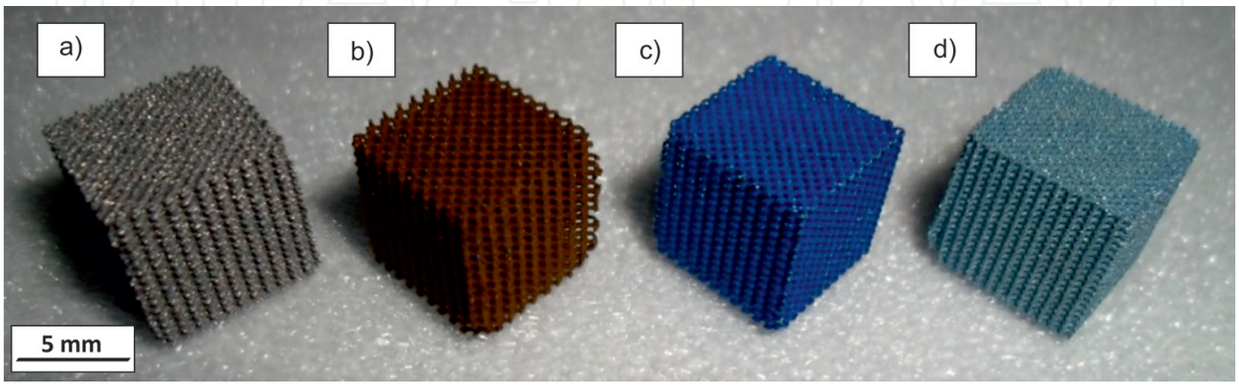

Figure 14. Cubic scaffolds viewed with a bare eye, including scaffolds without surface treatment (a) and scaffolds coated with TiO_2 layer during 550 (b), 1050 (c) and 1550 (d) cycles.

http://dx.doi.org/10.5772/65375

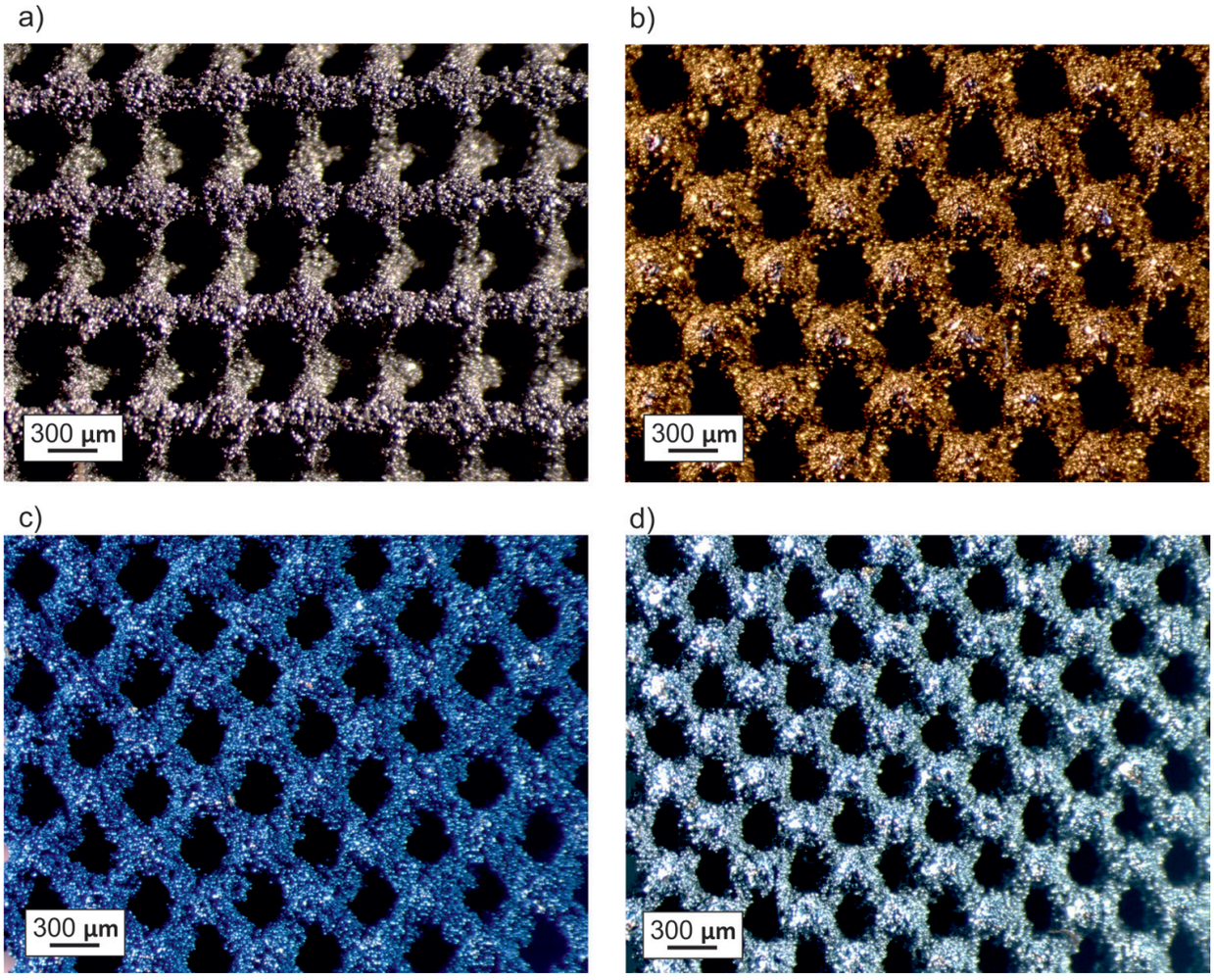

Figure 15. Stereoscopic images of scaffolds, including scaffold without surface treatment (a) and scaffolds coated with TiO_2 layer during 550 (b), 1050 (c) and 1550 (d) cycles.

observed with a bare eye (**Figure 14**) and in a light stereoscopic microscope (**Figure 15**). The uncoated element, with silver-metallic colour, undergoing surface treatment with ALD becomes, successively: brown-gold (550 cycles), dark blue (1050 cycles) and light blue with silver shade (1550 cycles).

The topography of scaffolds' surface coated with layers deposited by ALD is distinct for their irregularities measured at a nanometric scale, the number of which is rising proportionally to the number of the deposited layers. In particular, a layer deposited in 550 cycles has a rather uniform granular structure and the larger clusters of atoms are occurring on it only occasionally. In the case of a layer deposited in 1050 cycles, clusters of atoms with the diameter of about 1 µm occur every several microns. The biggest clusters of atoms, forming 'islands' with the length of up to several microns, exist in the case of a layer deposited in 1550 cycles, as shown in **Figure 16**.

The nanometric thickness of titanium dioxide layers deposited by ALD results in the fact that the layers deposited can be observed in a scanning electron microscope only for very high

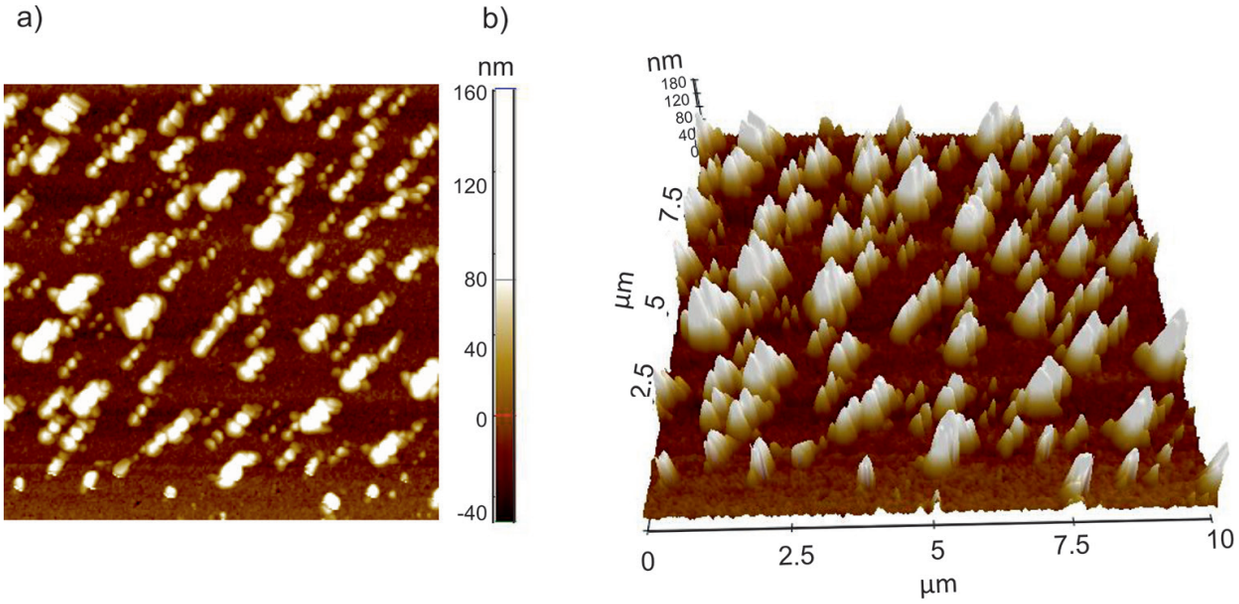

Figure 16. AFM image of surface topography of layer deposited in 1,550 cycles: (a) 2D; (b) 3D.

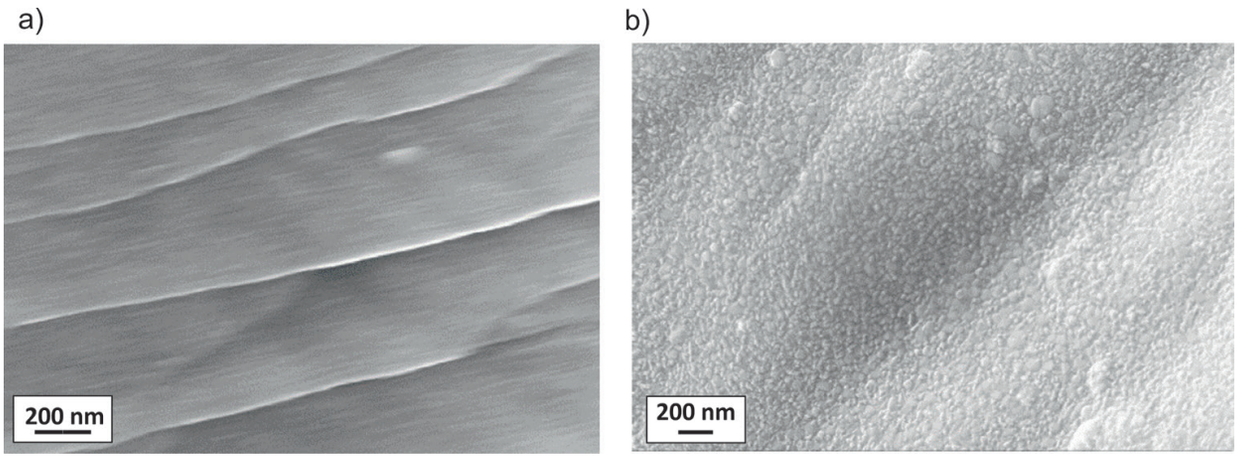

Figure 17. SEM image of scaffold surface: (a) without surface treatment; (b) with TiO_2 layer deposited in 1550 cycles.

magnifications of 150 kx. A clear difference between a scaffold surface without surface treatment (**Figure 17**) and scaffold surface covered with a TiO_2 layer in ALD (**Figure 17b**) can be observed only when such high magnifications are used. The scaffold surface, immediately following fabrication, is smooth with clear longitudinal bands arranged every several dozens of nanometres, corresponding to the laser activity direction. The deposited atomic TiO_2 layer, when magnified 150 kx, is visible as a 'sheep', i.e. a set of numerous adjacent oval granules of which only few have larger diameter.

6. Conclusions

Currently, there is a high social demand for individualised implants, which would significantly improve the quality of life of patients with partial palate losses caused by mechanical injuries, tumorous diseases or cleft palate. The methods currently in use, such as metallic or

polymeric prostheses, do not meet users' expectations as they often lack durability, convenience and aesthetics. A porous scaffold with its dimensions and shape perfectly suited to a patient plate loss made of a biocompatible material (Ti or Ti6AlV4) and additionally coated with a nanometric layer of osteoconductive titanium oxide seems to be a breakthrough solution. Modern CAMD software allows converting data acquired at a clinical stage into a 3D solid model of a palate loss piece. The model is then converted into a porous model through the multiplication of a unit cell whose dimensions and shape may be designed according to a patient's individual preferences. The pores existing in the material structure have the diameter of approx. 500 μm and should be open, because a scaffold, in its intended conditions of use, is to grow through a patient's living tissue. The experiments made confirm that the selective laser melting technology allows, following process conditions' optimisation, to produce biomimetic objects with a structure featuring open pores, as this was confirmed in microscopic (SEM) examinations. The objects have sufficiently good mechanical properties such as bending and compressive strength, which are similar to the properties of a cortical bone. The biotolerance and osteoconduction of laser-sintered scaffolds can be additionally improved through surface treatment allowing to cover a complex geometrical surface, such as a porous scaffold structure, uniformly from all sides. The treatment is carried out by the deposition of atomic layers and the deposited layer is 50–150 nm thick depending on the number of cycles.

Acknowledgements

All the results, images and detailed diagrams presented in this chapter have been developed in the framework of the BIOLASIN project entitled 'investigations of structure and properties of newly created porous biomimetic materials fabricated by selective laser sintering' headed by Prof. L.A. Dobrzański, funded by the Polish National Science Centre in the framework of the 'Harmony 4' competitions. The project was awarded a subsidy under the decision DEC-2013/08/M/ST8/00818.

Author details

Leszek A. Dobrzański[1]*, Anna D. Dobrzańska-Danikiewicz[1], Anna Achtelik-Franczak[1], Lech B. Dobrzański[2], Marek Szindler[1] and Tomasz G. Gawel[1]

*Address all correspondence to: leszek.adam@gmail.com

1 Faculty of Mechanical Engineering, Silesian University of Technology, Gliwice, Poland

2 Centre of Medicine and Dentistry SOBIESKI, Gliwice, Poland

References

[1] A. Nouri, P.D. Hodgson, C. Wen. Biomimetic Porous Titanium Scaffolds for Orthopedic and Dental Applications. In: M. Amitava, editor. Biomimetics learning from nature. Rijeka, Croatia: InTech; 2010. pp. 415–450.

[2] S.W. Kim, H.D. Jung, M.H. Kang, H.E. Kim, Y.H. Koh, Y. Estrin. Fabrication of porous titanium scaffold with controlled porous structure and net-shape using magnesium as spacer. Materials Science and Engineering C. 2013;33(5):2808–2815. DOI: 10.1016/j.msec.2013.03.011

[3] Y. Wang, Y. Shen, Z. Wang, J. Yang, N. Liu, W. Huang. Development of highly porous titanium scaffolds by selective laser melting. Materials Letters. 2010;64(6):674–676. DOI: 10.1016/j.matlet.2009.12.035

[4] G. Ryan, A. Pandit, D.P. Apatsidis. Fabrication methods of porous metals for use in orthopaedic applications. Biomaterials. 2006;27(13):2651–2670. DOI: 10.1016/j.biomaterials.2005.12.002

[5] S.J. Simske, R.A. Ayers, T.A. Bateman. Porous materials for bone engineering. Materials Science Forum. 1997;250:151–182. DOI: 10.4028/www.scientific.net/MSF.250.151

[6] L.M.R. de Vasconcellos, M.V. de Oliveira, M.L. de Alencastro Graça. Porous titanium scaffolds produced by powder metallurgy for biomedical applications. Materials Research. 2008;11(3):275–280. DOI: 10.1590/S1516-14392008000300008

[7] Z. Esen, S. Bor. Processing of titanium foams using magnesium spacer particles. Scripta Materialia. 2007;56(5):341–344. DOI: 10.1016/j.scriptamat.2006.11.010

[8] M. Bram, H. Schiefer, D. Bogdański, M. Köller, H.P. Buchkremer, D. Stöver. Implant surgery: How bone bonds to PM titanium. Metal Powder Report. 2006;61(2):26–31. DOI: 10.1016/S00260657

[9] S. Kumar. Selective laser sintering: A qualitative and objective approach. Modeling and Characterization. 2003;55(10):43–47.

[10] W. Xue, B.V. Krishna, A. Bandyopadhyay, S. Bose. Processing and biocompatibility evaluation of laser processed porous titanium. Acta Biomaterialia. 2007;3(6):1007–1018. DOI: 10.1016/j.actbio.2007.05.009

[11] M. Bram, C. Stiller, H.P. Buchkremer, D. Stover, H. Baur. High-porosity titanium, stainless steel and superalloy parts. Advanced Engineering Materials. 2000;2(4):196–199. DOI: 10.1002/(SICI)1527-2648(200004)2:4<196::AID-ADEM196>3.0.CO;2-K

[12] B. Dąbrowski, W. Świeszkowski, D. Godliński, K.J. Kurzydlowski. Highly porous titanium scaffolds for orthopaedic applications. Journal of Biomedical Materials Research Part B: Applied Biomaterials. 2010;958(1):53–61. DOI: 10.1002/jbm.b.31682

[13] R.C. Thomson, M.C. Wake, M.J. Yaszemski, A.G. Mikos. Biodegradable polymer scaffolds to regenerate organs. Advances in Polymer Science. 2005;122:245–274.

[14] L.S. Bertol, W.K. Júnior, F.P. da Silva, C.A. Kopp. Medical design: Direct metal laser sintering of Ti-6Al-4V. Materials & Design. 2010;31(8):3982–3988. DOI: 10.1016/j.matdes.2010.02.050

[15] L. Lu, J. Fuh, Y. Wong. Laser Induseed Materials and Processes for Rapid Prototyping. In: L. Lu et al., editor. Laser-induced materials and prosesses for rapid prototyping. Dordrecht: Kluwer Publishers; 2001. pp. 89–142.

[16] L. Ciocca, M. Fantini, F. de Crescenzio, G. Corinaldesi, R. Scotti. Direct metal laser sintering (DMLS) of a customized titanium mesh for prosthetically guided bone regeneration of atrophic maxillary arches. Medical & Biological Engineering & Computing. 2011;49:1347–1352.

[17] A. Mazzoli. Selective laser sintering in biomedical engineering. Medical & Biological Engineering & Computing. 2012;51(3):245–256.

[18] A. Bandyopadhyay, F. Espana, V.K. Balla, S. Bose, Y. Ohgami, N.M. Davies. Influence of porosity on mechanical properties and in vivo responseof Ti6Al4V implants. Acta Biomaterialia. 2010;6(4):1640–1648. DOI: 10.1016/j.actbio.2009.11.011

[19] S. van Bael, Y.C. Chai, S. Truscello, M. Moesen, M. Moesen, G. Kerckhofs, H van Oosterwyck, J.P. Kruth, J. Schtooten. The effect of pore geometry on the in vitro biological behavior of human periosteum-derived cells seeded on selective laser-melted Ti6Al4V bone scaffolds. Acta Biomateralia. 2012;**8**(7):2824–2834. DOI: 10.1016/j.actbio.2012.04.001

[20] I. Shishkovsky, V. Scherbakov. Selective laser sintering of biopolymers with micro and nano. Physics Procedia. 2012;**39**:491–499. DOI: 10.1016/j.phpro.2012.10.065

[21] EN ISO 5832-3:2012. Implants for surgery – Metallic materials – Part 3: Wrought titanium 6-aluminium 4-vanadium alloy (ISO 5832-3:1996), ISC 11.040.40, European Committee for Standardization (CEN), Brussels, Belgium 2012.

[22] R. Melechow, K. Tubielewicz, W. Błaszczyk, editors. Titanium and its alloys: types, properties, applications, processing technology, degradation (in Polish). Częstochowa: PC Publishing; 2004.

[23] L.A. Dobrzański, editors. Fundamentals of materials science (in Polish). Gliwice: Publishing of Silesian University of Technology; 2012.

[24] L.A Dobrzański, Descriptive physical metallurgy of non-ferrous alloys, Silesian University of Technology Publishing, Gliwice, Poland; 2009 (in Polish).

[25] L.A. Dobrzański, A.D. Dobrzańska-Danikiewicz, A. Achtelik-Franczak, L.B. Dobrzański. Comparative analysis of mechanical properties of scaffolds sintered from Ti and Ti6Al4V powders. Archives of Materials Science and Engineering. 2015;**73**(2):69–81.

[26] G. Pyka, A. Burakowski, G. Kerckhofs, M. Moesen, S. V. Bael, J. Schrooten, M. Wevers. Surface modification of ti6al4v open porous structures produced by additive manufacturing. Advanced Engineering Materials.2012;**14**(6):363–370. DOI: 10.1002/adem.201100344

[27] L.A. Dobrzański, A. Achtelik-Franczak, M. Król. Computer aided design in Selective Laser Sintering (SLS)—application in medicine. Journal of Achievements in Materials and Manufacturing Engineering. 2013;**60**(2):66–75.

[28] M. Król, L.A. Dobrzański, Ł. Reimann, I. Czaja. Surface quality in selective laser melting of metal powders. Archives of Materials Science and Engineering.2013;**60**(2):87–92.

[29] L.A. Dobrzański, A.D. Dobrzańska-Danikiewicz, P. Malara, T.G. Gaweł, L.B. Dobrzański, A. Achtelik-Franczak. Fabrication of scaffolds from TI6AL4V powders using the computer aided laser method. Archives of Metallurgy and Materials. 2015;**60**(2):1065–1070. DOI: 10.1515/amm-2015-0260

[30] T. Węgrzyn, J. Piwnik, B. Łazarz, R. Wieszała, D. Hadryś. Parameters of welding with micro-jet cooling. Archives of Materials Science and Engineering. 2012;**54**(2):86–92.

[31] A. Sękala, G. Ćwikła, G. Kost. The role of multi-agent systems in adding functioning of manufacturing robotized cells. In: IOP Conf. Series: Materials Science and Engineering 95, editors. ModTech; Romania. Romania: IOP Publishing Ltd; 2016. p. 012097.

[32] A. Sękala, A. Gwiazda, K. Foit, W. Banaś, P. Hryniewicz, G. Kost.Agent-based models in robotized manufacturing cells designing. In: IOP Conf. Series: Materials Science and Engineering 95, editors. ModTech; Roamnia. Romania: IOP Publishing Ltd; 2015. p. 012106.

[33] A. Kaźnica, R. Joachimiak, T. Drewa, T. Rawo, J. Deszczyński. New trends in tissue engineering. Arthroscopy and Arthritis Surgery. 2007;3(3):11–16 (in Polish).

[34] N. Evans, E. Gentelman, J. Polak. Scaffolds for stem cells. Materials Today.2006;**9**(12): 26–33. DOI: 10.1016/S13697021

[35] T. Węgrzyn, R. Wieszała. Significant alloy elements in welded steel structures of car body. Archives of Metallurgy and Materials. 2012;**57**(1):45–52. DOI: 10.2478/v10172-011-0151-4

[36] L.A. Dobrzański, A.D. Dobrzańska-Danikiewicz, P. Malara, T.G. Gaweł, L.B. Dobrzański, A. Achtelik. Patent Application No. 414423. Polish Patent Office. 2015.

[37] A. Laptev, O. Vyal, M. Bram, H.P. Buchkremer, D. Stöver. Green strength of powder compacts provided for production of highly porous titanium parts. Powder Metallurgy. 2005;**48**(4):358–364. DOI: 10.1179/174329005X73838

[38] G. Budzik, D. Pająk, M. Magniszewski, W. Budzik. Rapid prototyping methods (in Polish). Steel Metals & New Technologies.2011;**1–2**:78–79.

[39] L.A. Dobrzański, R. Nowosielski, E. Hajduczek, editors. Research methods of metals and their alloys: Light and electron microscopy (in Polish). 2nd ed. Warszawa: WNT; 1987.

[40] J. Nowacki, L.A. Dobrzański, F. Gustavo, editors. Implants in the intramedullary osteosynthesis of long bones (in Polish). Gliwice: Open Access Library; 2012. 150 p.

[41] A. Mahapatro. Bio-functional nano-coatings on metallic biomaterials. Materials Science and Engineering: C. 2015;**55**:227–251. DOI: 10.1016/j.msec.2015.05.018

[42] E.O. López, A.L. Rossi, B.S. Archanjo, R.O. Ospina, A. Mello, A. M. Rossi. Crystalline nano-coatings of fluorine-substituted hydroxyapatite produced by magnetron sputtering with high plasma confinement. Surface and Coatings Technology. 2015;**264**:163–174. DOI: 10.1016/j.surfcoat.2014.12.055

[43] L A. Dobrzański, L. Reimann. Influence of Cr and Co on hardness and corrosion resistance CoCrMo alloys used on dentures. Journal of Achievement in Materials and Manufacturing Engineering. 2011;**49**(2):193–199.

[44] L.A. Dobrzański, A.D. Dobrzańska-Danikiewicz, M. Szindler, A. Achtelik-Franczak, W. Pakieła. Atomic layer deposition of TiO2 onto porous biomaterials. Archives of Materials Science and Engineering. 2015;**75**(1):5–11.

IntechOpen